RSC Advances

PAPER

View Article Online
View Journal | View Issue

Cite this: *RSC Adv.*, 2022, **12**, 30921

A realistic perspective for CO_2 triggered tuning of electrical conductivity†

Mizaj Shabil Sha, [a] Bijandra Kumar, [b] Aboubakr M. Abdullah,[a] Suresh Muthusamy[c] and Kishor Kumar Sadasivuni *[a]

Received 1st September 2022
Accepted 23rd October 2022

DOI: 10.1039/d2ra05511b

rsc.li/rsc-advances

To seek sustainable CO_2 sequestration and conversion, an electrochemical cell has been investigated for carbon capture and utilization strategy (CCU). In this cell, atmospheric CO_2 is captured under ambient conditions and incorporated into power generation using zinc nanopowder as the catalyst. As a result, a method was developed to tune the electronic property of zinc by passing CO_2. It was observed that nearly three orders of magnitude of conductivity could be changed along with achieving a carbon capture strategy. The system also exhibited good stability. In this process, it was observed that efficient current generation could be achieved due to zinc's active participation as a catalyst. The detailed physicochemical characterizations of catalysts were also examined. XRD, FTIR and TEM analysis perform the structural and morphological characterization. The system performance was further investigated using different criteria.

1 Introduction

The Intergovernmental Panel on Climate Change (IPCC) recently concluded that rising CO_2 concentrations from fossil fuel use and deforestation are responsible for most observed global warming.[1,2] Not only have civilization and industrialization provided technology, contemporary life, and convenience, but they have also brought pollution and emissions from industries, cars, and chemical plants.[3,4] According to the International Energy Agency (IEA)-World Energy Outlook (WEO), depending on current policies, CO_2 emissions will be 63% greater by 2030 than they are today, or over 90% higher than they were in 1990.[5,6]

As a result, improved activities than those currently being implemented by governments are required to avert further rises over the next few decades, including developing and implementing technology solutions to reduce CO_2 emissions significantly.[7] One such alternative is to trap CO_2 from big sources such as thermal power plants (where each tonne of coal burned produces around 4 tonnes of CO_2) and prevent it from entering the atmosphere by appropriately capturing, storing, and converting it into useful chemicals/fuels.[8,9] At the moment, the widely available solution to address the CO_2-related global warming problem is CO_2 capture and storage (CCS) at safe locations.[10,11] In comparison to CCS, CO_2 collecting and recycling (CCR) has been regarded as the most promising solution. Aside from economic gains, the socio-political benefits include a favorable image for corporations who embrace programs to reuse CO_2 created by fossil fuels.[12,13]

One of the most crucial components in the battery industry is zinc. Zn has been used extensively in primary batteries for millennia because of its high energy density, low cost, high availability on Earth, low toxicity, and relatively simple manufacturing procedure.[14] Light-emitting diodes, flexible electronics, solar cells, driving circuits for liquid crystal displays (LCDs), and organic light-emitting diode TVs are just a few of the numerous uses of zinc. Numerous advances have been achieved in studying cathode materials since the discovery of reversible zinc-ion storage in an aqueous solution.[15] Although commercial zinc foil has been utilized in anode materials, and not much has been done to address its inherent drawbacks.[16] The usage of zinc metal anodes has gained increased attention during the last two years, with various studies outlining problems and proposing pertinent improvements.[17–19]

It is desirable to adjust the electrical conductivity of materials for various applications, including switches, sensors, condensers, and variable resistors, and different methods are used for tuning. Enhanced electrical conductivity of ZnO film may improve the performance of the electron-conductive ZnO layer for various applications. By introducing a variety of methods of doping, several studies have focused on improving the electrical conductivities of ZnO films.[20] Temperature limitation for usage is one major disadvantage associated with thermal tuning. As a result, chemical tuning is preferred over thermal tuning.

[a]*Center for Advanced Materials, Qatar University, P. O. Box 2713, Doha, Qatar. E-mail: kishor_kumars@yahoo.com*

[b]*Department of Technology, Elizabeth City State University, Elizabeth City, USA*

[c]*Department of Electronics and Communication Engineering, Kongu Engineering College (Autonomous), Perundurai, Erode, Tamilnadu, India*

† Electronic supplementary information (ESI) available. See DOI: https://doi.org/10.1039/d2ra05511b

In most cases, dissolving and expelling CO_2 is preferred for chemical tuning since it is more repeatable, safe, and environmentally benign than chemical reagents. Previous reports suggest that Zn can be a powerful reducing agent for CO_2.[21,22] As per the literature, we have found that there is a possibility that CO_2 is captured by glucose solution and it is converted to zinc carbonates.[21] Literature suggests that organic compounds containing alcohol groups, such as isopropanol, glycerol, glucose, C2 and C3 alcohols, saccharides and lignin derivatives, are often used as reductants. Carrying out the hydrolysis of biomass simultaneously with the reduction of CO_2 captured as a basic solution (*i.e.*, bicarbonate, amine carbamates of ammonia) could be interesting because many of the hydrolysis products of biomass contain alcohol groups that can act as reductants of CO_2.[22]

No reports of tuning by CO_2 with transition-type solid conductors in the presence of carbohydrates have been made up until this point. Shifting molecular structures between neutral and ionic species can be used to tune by CO_2 bubbling in a solution.[23]

In this study, we have developed experiments showing how a release of CO_2 influences electrical conductivity. We examined that by passing CO_2, the current of Zn can be adjusted three times over.

2 Materials and experiments

2.1. Chemicals

E. Merck provided zinc acetate dihydrate ($Zn(CH_3COO)_2 \cdot 2H_2O$). Fisher Scientific U.K. Limited (U.K.) provided D-glucose anhydrous. Thermo Fisher Scientific (U.S.A.) and AMWAY (India) provided Nafion and NaOH, respectively. All the chemicals were utilized without further purification. A Millipore-Q deionized (DI) water purification system provided the required water throughout the experiments.

2.2. Synthesis of zinc nanoparticle

0.189 millimolar zinc acetate dihydrate ($Zn(CH_3COO)_2 \cdot 2H_2O$) was prepared with distilled water. 0.875 millimolar sodium hydroxide (NaOH) was prepared and added dropwise to the zinc acetate solution until pH was maintained at 12. The mixture was stirred for 1 h until the precipitate was obtained. The residue was washed using deionized water, filtered, and dried overnight in the hot air oven at 70 °C. ZnO is heated with crushed coke at 1673 K, where it is reduced to Zn.

2.3. Characterization techniques

Numerous morphological and structural analyses were conducted on the Zn nanoparticles. Crystallinity was examined using an X-ray diffractometer (X'PERT-Pro M.P.D., PANalytical Co., Almelo, Netherlands). Transmission electron microscopy was used to investigate the morphology of the nano powder. Thermo Nicolet Nexus 670 FTIR spectrometer analyzed the purity of nano powder.

2.4. Electrochemical experiments

Electrochemical experiments were performed using a three-electrode system. The counter, working electrode, and reference were graphite rod, glassy carbon (diameter 3 mm), and Ag/AgCl (3 M KCl solution). A mixture of 20 mg of zinc nano powder, 2 ml of ethanol and 20 μL of Nafion solution was ultrasonicated to produce homogeneous catalytic ink. The working electrode was polished using aluminium oxide powder and cleaned using distilled water. Afterward, 10 μL of catalytic ink was uniformly coated on the surface of GCE and dried under ambient conditions. Electrochemical measurements were carried out by Gamry potentiostat/galvanostat (Ref 600) using 20% basic glucose solution as an electrolyte. Cyclic voltammetry (CV), electrochemical impedance spectroscopy (EIS) were carried out at specific parameters. The potential range was −1 to 1 V *vs.* reference electrode, with the sweep rate varying from 50 to 200 mV s^{-1}.

3 Results and discussion

3.1. Structural analysis

Fig. 1a depicts the XRD patterns of zinc nanoparticles. The peaks at 2θ values of 36.3280°, 39.0324°, 43.2562°, 54.3599°, 70.1174°, 77.1101°, 82.1218°, and 89.9488°, are indexed to the (002), (100), (101), (102), (103), (110), and (004) planes, respectively, of the zinc (JCPDS 98-042-1014).[24] XRD plot authenticates hexagonal crystal structures of metallic Zn. Small peaks indicating the presence of ZnO_2 were also observed. The crystallite size (D) is calculated using the Debye–Scherrer equation and found as 35 nm. As per the XRD results, the Zn nanoparticles exhibit high crystallinity due to their very sharp diffraction peaks.

FTIR spectra of zinc nanoparticles for determining purity at wavenumber 400–4000 cm^{-1} are represented in Fig. 1b. Furthermore, the FTIR spectrum of the synthesized Zn NPs showed a sharp and intense band at 756 cm^{-1}, indicating the existence of Zn–O vibration.[25] This may corresponds to the surface oxidation.

3.2. Transmission electron microscopy (TEM) analysis

The structural and morphological characterizations were explored by TEM analysis. Selected area diffraction (SAED) patterns were also used to observe the morphology and crystallinity by high-resolution transmission electron microscopy (Tecnai G2 S Twin F20 (200 kV FEG) FEI). Fig. 2 represents the TEM images of zinc nanoparticles (Fig. 2a) and the catalytic ink (Fig. 2b). TEM images confirm the presence of several nanoparticle aggregates along with some individual crystals (Fig. 2a(i) and b(i)). These clearly show that zinc nanoparticles exhibit a polycrystalline structure. Even though these particles tend to overlap, the overall dispersion effect can be considered excellent (Fig. 2a(ii) and b(ii)). Fig. 2a(iii) and b(iii) represent the SAED pattern of zinc nanoparticles and the catalytic ink, respectively. Electron diffraction (SAED) pattern polycrystallinity of the nanoparticles is verified from the corresponding selected area.

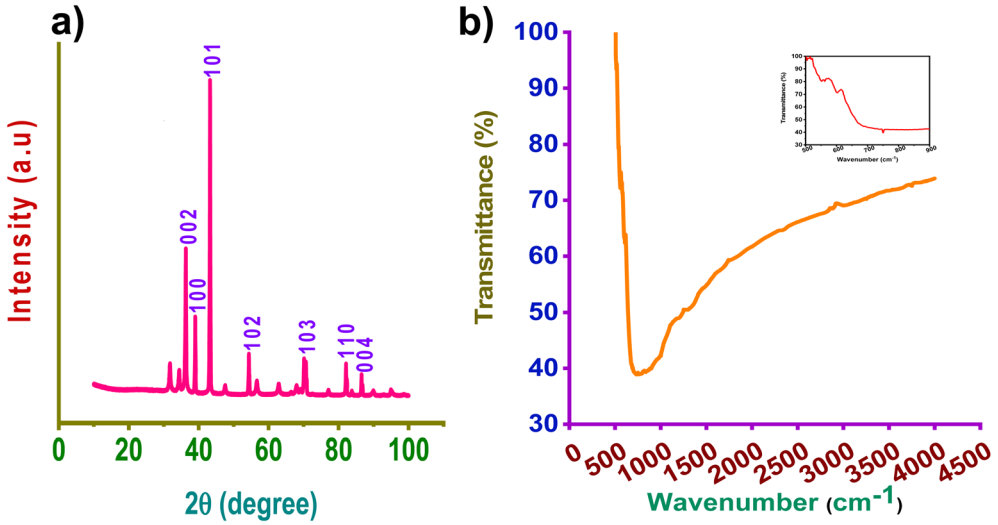

Fig. 1 (a) XRD pattern of zinc nanoparticles and (b) FTIR spectrum, insight represents FTIR representing the sharp and intense band.

3.3. Electrochemical analysis

3.3.1 Sensing performance-effect of CO_2. The electrochemical kinetics of the zinc nano powder for CO_2 embedded glucose cells was investigated by cyclic voltammetry (CV) at ambient temperature and pressure. A 20% basic glucose solution (pH 10) was used as an electrolyte for the analysis. We also evaluated the performance in different electrolytes, water, NaOH and neutral glucose solution (ESI Fig. 1†). Fig. 3b shows the CV plot at sweeping rates of 50–200 mV s^{-1}.

Fig. 3a shows the CV measured for a glucose cell using a zinc CO_2 saturated solution and a CO_2 unsaturated solution. From the figure, it can be observed that after passing CO_2, the current density has increased dramatically. The chances of oxidation of the Zn metal surface are high when immersed in aqueous electrolytes. And this can be controlled by manipulating the redox reaction, which further influences CO_2 capturing.[26] Fig. 3b shows the CV measured during the process by varying sweeping rates from 50 and 200 mV s^{-1} in CO_2 saturated solution, respectively. During measurements, it was observed that current density shot up rapidlywhen the scan rate varied from 50 to 100 mV s^{-1}, afterward slightly increased for further increase in the scan rate.

The CV response of various CO_2 flow rates in basic glucose solution was also investigated (Fig. 3c). The influence of CO_2 flow rate on overall current density is depicted in Fig. 3a. As previously stated, the current density is slightly affected by the CO_2 flow rate.[27]

The system's performance in the nitrogen atmosphere was also evaluated (Fig. 3d). Compared to N_2, the cyclic voltammogram revealed the greatest produced currents for the CO_2 period at any applied potential, indicating its quick reaction kinetics (Fig. 3a and d).

3.3.2 Evaluation of performance based on different criteria. CO_2 saturated glucose cell performance was investigated using different criteria (Fig. 4). The electrolyte's pH was considered one of the criteria, and the experiments were conducted in electrolytes having different pHs (Fig. 4a). The basic glucose solution was observed to have excellent performance compared to the neutral and acidic solutions. It was also noticed that neutral glucose solution has the least affinity towards the reaction. These results indicate that alkaline (pH 10) glucose reduces mass transfer resistance.[28]

Additionally, the effect of zinc loading amount and obtained results are presented in Fig. 4b. It can be seen that the current density increases gradually with an increase in the loading amount to 25 mg and remains constant afterward. This trend in current density could be elaborated based on the decrease in surface area due to the accumulation of nanoparticles which are not conducive to an efficient catalysis process.[29] The maximum current density was achieved when the zinc loaded was 25 mg. Hence, a 25 mg catalyst was used for further experiments. It was observed that current density and amount of zinc loaded follows an exponential relationship $Y = Y_0 + A_1(1 - \exp^{(-x/t_1)}) + A_2(1 - \exp^{(-x/t_2)})$ with parameters $Y_0 = -0.18754 \pm 9.73818$, $A_1 = 1.3634 \pm 3.72229 \times 10^6$, $t_1 = 6.80887 \pm 1.22557 \times 10^6$, $A_2 = 1.3634 \pm 3.72229 \times 10^6$ and $t_2 = 6.8088 \pm 1.2256 \times 10^6$. The squared regression coefficient (R^2) was 0.89789.

The effect of glucose concentration on performance was investigated. It was observed that current density increases when the glucose concentration increases from 5 to 20% and remains constant afterward (Fig. 4c). Excessive glucose molecules may lead to covering the electrode surface, preventing further oxidation. Additionally, the high concentration of glucose molecules may prevent H^+ from leaving the electrode surface, eventually lowering the electrode's power density.[28] In this experiment, a 20% glucose solution controlled enough molecules to cover the electrode surface completely.

3.3.3 Repeatability and sensing consistency of zinc nanoparticles. Stability assessments for electrocatalytic CO_2 capturing by zinc nanoparticles were analyzed *via* cyclic voltammetry for 500 cycles in the CO_2-saturated basic glucose solution for a sweep rate of 100 mV s^{-1}. Interestingly, higher

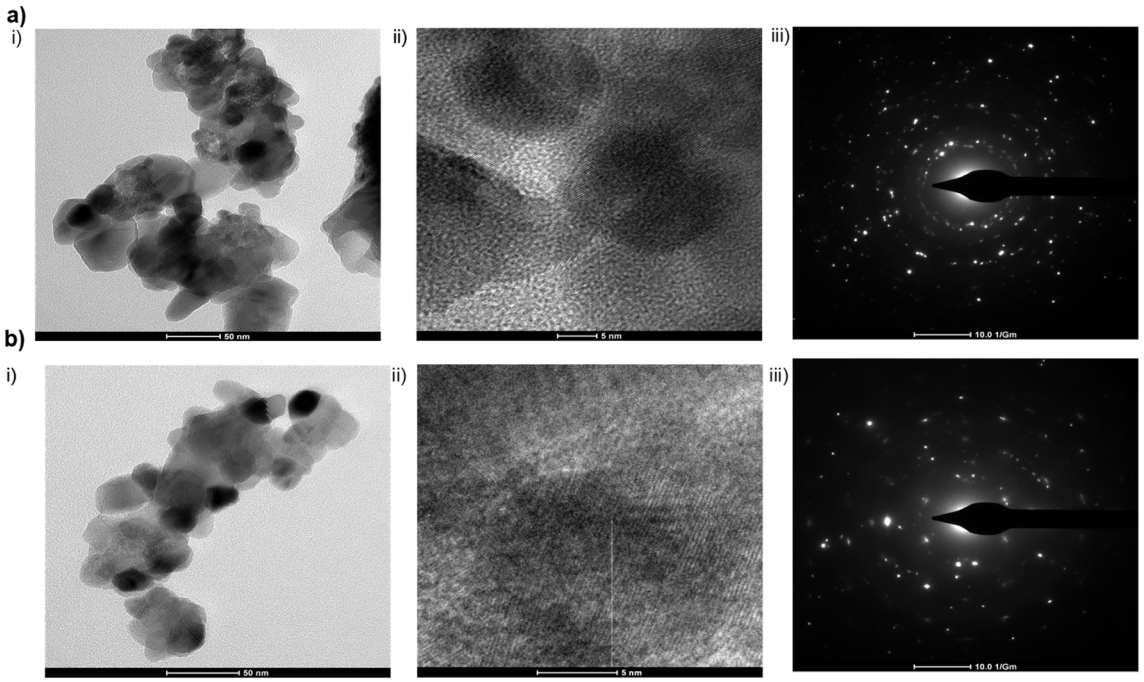

Fig. 2 TEM images of (a) zinc nanoparticles and (b) catalytic ink. (i) Crystalline structure, (ii) dispersion of particles (iii) SAED pattern, respectively.

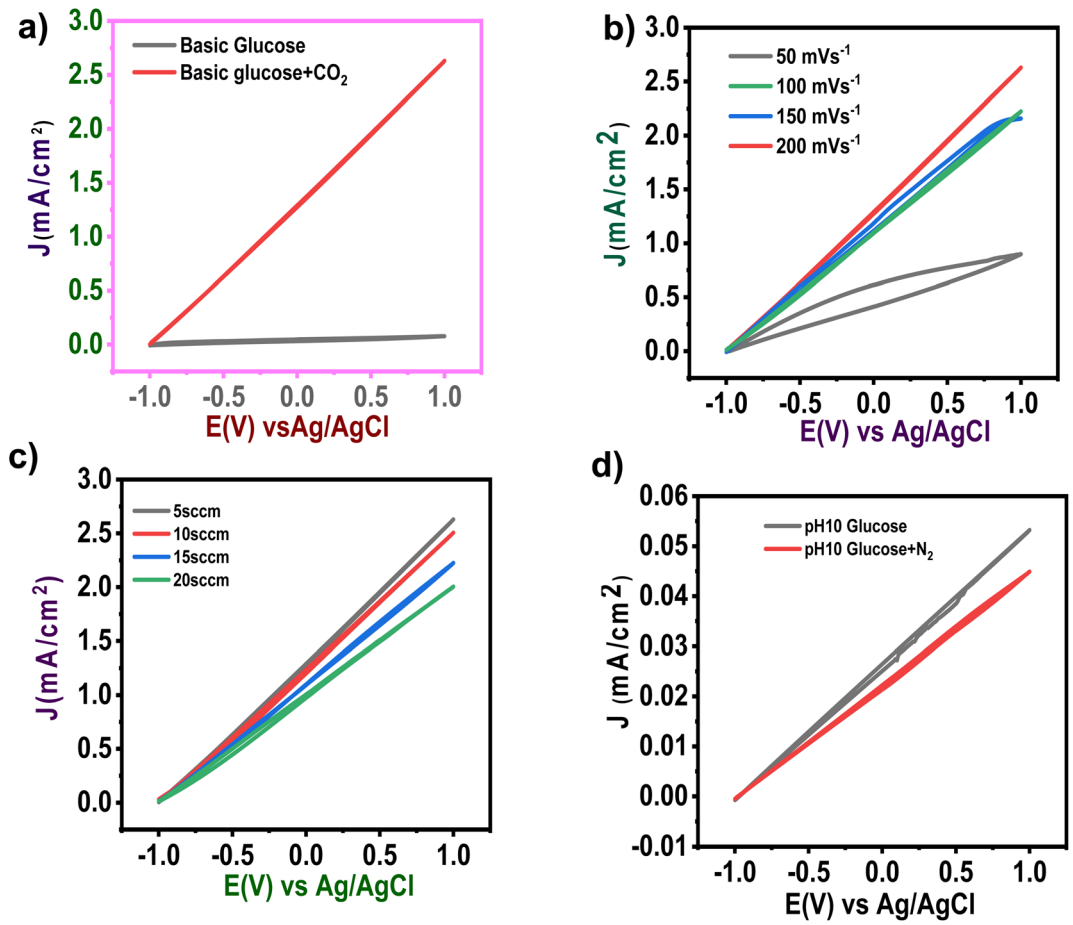

Fig. 3 Cyclic voltammetry plots for glucose cell (a) with and without CO_2 (b) effect of scan rate in CO_2 saturated glucose cell (c) CV curves obtained at different gas flow rates of CO_2 (scan rate 50 mV s^{-1}) (d) with and without N_2.

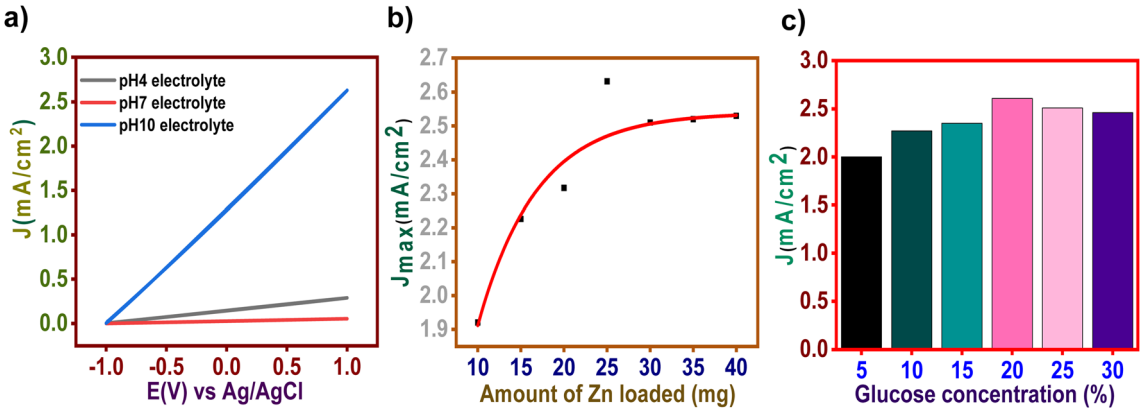

Fig. 4 Evaluation of the performance of CO_2 saturated glucose cell (a) pH effect (b) effect of zinc loading (c) effect of glucose concentration.

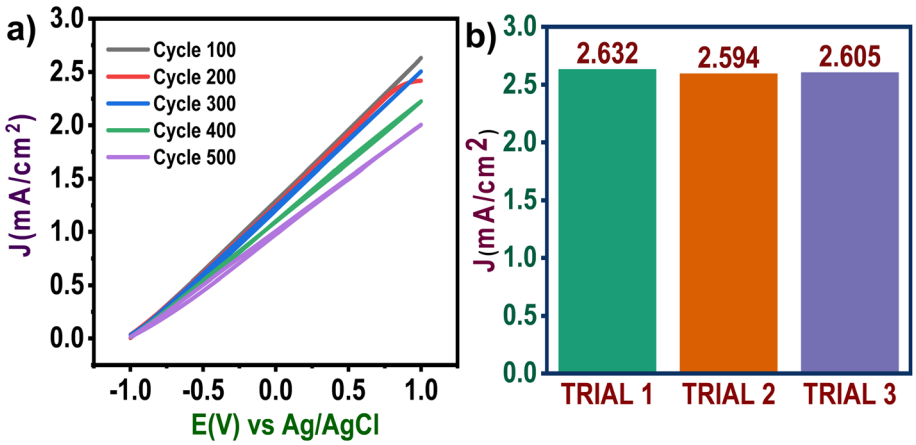

Fig. 5 Stability analysis (a) repeatability (b) sensing consistency.

retention of the current was observed even after 500 cycles, with a slight current variation manifesting the greater stability of zinc nanoparticles as a catalyst for the glucose cell (Fig. 5a).

Following this, we also evaluated the sensing consistency of zinc nanoparticles for adapting to real-life applications. For this purpose, CV measurement was carried out at 100 mV s^{-1} for 100 cycles, and after that, the electrolyte was replaced. Then CV measurements were carried out again to check the consistency of zinc nanoparticles as electrocatalysts (Fig. 5b). It was observed that zinc possesses excellent consistency in sensing CO_2-saturated glucose solutions.

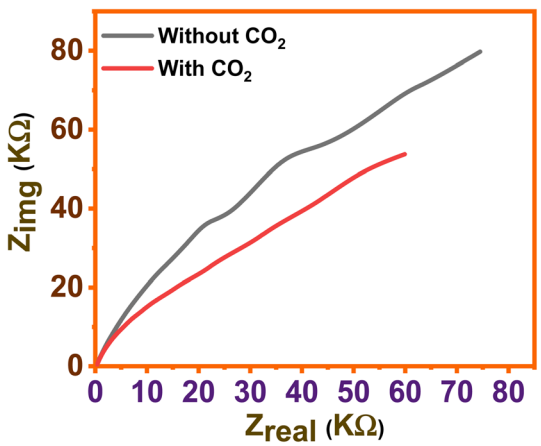

Fig. 6 EIS spectra of CO_2 saturated and unsaturated solution.

3.3.4 Electrochemical impedance spectroscopy (EIS). The impedance spectroscopy (EIS) measurements were carried out in electrolyte solution with and without CO_2 saturation to investigate further charge transfer and ion transportability across the zinc electrode and electrolyte interface (Fig. 6). However, because of the electrode's surface area, neither of the Nyquist plots shows a discernible semicircle indicating a low impedance. The ease with which electrons may move across the electrode surface reduces the charge transfer resistance in the high-frequency zone.[29] The charge-transfer resistance value of the CO_2-saturated electrolyte was lower than that of the unsaturated electrolyte, which was associated with the surface morphology of Zn NPs, which captured CO_2. Introducing CO_2 on the surface of zinc nanoparticles has decreased the resistance for charge transfer during the electrochemical reaction. The film capacitance of the CO_2-captured electrode was higher

than that of the bare electrode. The results revealed that the CO_2-captured electrode had better conductivity and charge storage capability.

4 Conclusion

In this work, electrochemical measurements were performed to investigate the impact of CO_2 while using a Zn catalyst. This study tried to fabricate electrochemical cells by integrating carbon dioxide, making this work unique. The performance of a nanostructured Zn cathode has been investigated to explore the potential application of CO_2 capturing for power generation. It was observed that the magnitude of the current generated was three times higher than without the presence of CO_2. The suggested cells are promising advancements that hold promise for a more practical application for energy sustainability powering implantable micro-devices. They are simple to produce on a large scale with relatively low cost and high repeatability. They can be preserved for long periods without suffering significant performance losses and are easy to preserve.

Author contributions

Mizaj Shabil Sha: data curation, formal analysis, investigation, methodology, writing – original draft Bijandra Kumar: writing – review & editing Aboubakr M. Abdullah: writing – review & editing Suresh Muthusamy: writing – review & editing Kishor Kumar Sadasivuni: conceptualization, supervision; validation, funding acquisition, project administration.

Conflicts of interest

The authors declare that they have no conflict of interest.

Acknowledgements

This work was carried out by the NPRP11S-1221-170116 from the Qatar National Research Fund (a member of the Qatar Foundation). The statements made herein are exclusively the accountability of the authors.

References

1 J. Tollefson, Carbon emissions rapidly rebounded following COVID pandemic dip, *Nature*, 2022, **19**(10), 6350.
2 J. Lelieveld, K. Klingmüller, A. Pozzer, R. T. Burnett, A. Haines and V. Ramanathan, Effects of fossil fuel and total anthropogenic emission removal on public health and climate, *Proc. Natl. Acad. Sci. U. S. A.*, 2019, **116**, 7192–7197.
3 Y. K. Dwivedi, L. Hughes, A. K. Kar, A. M. Baabdullah, P. Grover, R. Abbas, D. Andreini, I. Abumoghli, Y. Barlette, D. Bunker, L. Chandra Kruse, I. Constantiou, R. M. Davison, R. De', R. Dubey, H. Fenby-Taylor, B. Gupta, W. He, M. Kodama, M. Mäntymäki, B. Metri, K. Michael, J. Olaisen, N. Panteli, S. Pekkola, R. Nishant, R. Raman, N. P. Rana, F. Rowe, S. Sarker, B. Scholtz, M. Sein, J. D. Shah, T. S. H. Teo, M. K. Tiwari, M. T. Vendelø and M. Wade, Climate change and COP26: Are digital technologies and information management part of the problem or the solution? An editorial reflection and call to action, *Int. J. Inf. Manag.*, 2022, **63**, 102456.
4 F. Wang, J. D. Harindintwali, Z. Yuan, M. Wang, F. Wang, S. Li, Z. Yin, L. Huang, Y. Fu, L. Li, S. X. Chang, L. Zhang, J. Rinklebe, Z. Yuan, Q. Zhu, L. Xiang, D. C. W. Tsang, L. Xu, X. Jiang, J. Liu, N. Wei, M. Kästner, Y. Zou, Y. S. Ok, J. Shen, D. Peng, W. Zhang, D. Barceló, Y. Zhou, Z. Bai, B. Li, B. Zhang, K. Wei, H. Cao, Z. Tan, L. Zhao, X. He, J. Zheng, N. Bolan, X. Liu, C. Huang, S. Dietmann, M. Luo, N. Sun, J. Gong, Y. Gong, F. Brahushi, T. Zhang, C. Xiao, X. Li, W. Chen, N. Jiao, J. Lehmann, Y.-G. Zhu, H. Jin, A. Schäffer, J. M. Tiedje and J. M. Chen, Technologies and perspectives for achieving carbon neutrality, *Innovation*, 2021, **2**, 100180.
5 T. Ahmad and D. Zhang, A critical review of comparative global historical energy consumption and future demand: The story told so far, *Energy Rep.*, 2020, **6**, 1973–1991.
6 H. Fuhr, The rise of the Global South and the rise in carbon emissions, *Third World Q.*, 2021, **42**, 2724–2746.
7 C. Freitag, M. Berners-Lee, K. Widdicks, B. Knowles, G. S. Blair and A. Friday, The real climate and transformative impact of ICT: A critique of estimates, trends, and regulations, *Patterns*, 2021, **2**, 100340.
8 P. Madejski, K. Chmiel, N. Subramanian and T. Kuś, Methods and Techniques for CO2 Capture: Review of Potential Solutions and Applications in Modern Energy Technologies, *Energies*, 2022, **15**, 887.
9 S. Moazzem, M. G. Rasul and M. M. K. Khan, *A Review on Technologies for Reducing CO_2 Emission from Coal Fired Power Plants*, IntechOpen, 2012.
10 E. Martin-Roberts, V. Scott, S. Flude, G. Johnson, R. S. Haszeldine and S. Gilfillan, Carbon capture and storage at the end of a lost decade, *One Earth*, 2021, **4**, 1569–1584.
11 K. Witte, Social Acceptance of Carbon Capture and Storage (CCS) from Industrial Applications, *Sustainability*, 2021, **13**, 12278.
12 H. Kameyama, K. Yoshizaki and I. Yasuda, Carbon Capture and Recycle by Integration of CCS and Green Hydrogen, *Energy Proc.*, 2011, **4**, 2669–2676.
13 M. Bhattacharya, S. Sebghati, R. T. VanderLinden and C. T. Saouma, Toward Combined Carbon Capture and Recycling: Addition of an Amine Alters Product Selectivity from CO to Formic Acid in Manganese Catalyzed Reduction of CO2, *J. Am. Chem. Soc.*, 2020, **142**, 17589–17597.
14 H. Wang, D. Yu, C. Kuang, L. Cheng, W. Li, X. Feng, Z. Zhang, X. Zhang and Y. Zhang, Alkali Metal Anodes for Rechargeable Batteries, *Chem*, 2019, **5**, 313–338.
15 Y. Zhao, Y. Zhu and X. Zhang, Challenges and perspectives for manganese-based oxides for advanced aqueous zinc-ion batteries, *InfoMat*, 2020, **2**, 237–260.
16 X. Wang, S. Zheng, F. Zhou, J. Qin, X. Shi, S. Wang, C. Sun, X. Bao and Z.-S. Wu, Scalable fabrication of printed Zn//

MnO2 planar micro-batteries with high volumetric energy density and exceptional safety, *Natl. Sci. Rev.*, 2020, **7**, 64–72.

17 P. Zhao, B. Yang, J. Chen, J. Lang, T. Zhang and X. Yan, A Safe, High-Performance, and Long-Cycle Life Zinc-Ion Hybrid Capacitor Based on Three-Dimensional Porous Activated Carbon, *Acta Phys.-Chim. Sin.*, 2020, **36**(2), 1904050.

18 L. Shan, Y. Wang, S. Liang, B. Tang, Y. Yang, Z. Wang, B. Lu and J. Zhou, Interfacial adsorption–insertion mechanism induced by phase boundary toward better aqueous Zn-ion battery, *InfoMat*, 2021, **3**, 1028–1036.

19 J. Huang, Guest Pre-Intercalation Strategy to Boost the Electrochemical Performance of Aqueous Zinc-Ion Battery Cathodes, *Acta Phys. -Chim. Sin.*, 2021, **37**(3), 2005020, **http://www.whxb.pku.edu.cn/EN/10.3866/PKU.WHXB202005020**.

20 J. Pilz, A. Perrotta, P. Christian, M. Tazreiter, R. Resel, G. Leising, T. Griesser and A. M. Coclite, Tuning of material properties of ZnO thin films grown by plasma-enhanced atomic layer deposition at room temperature, *J. Vac. Sci. Technol., A*, 2018, **36**, 01A109.

21 F. Mani, M. Peruzzini and F. Barzagli, The role of zinc(II) in the absorption-desorption of CO2 by aqueous NH3, a potentially cost-effective method for CO2 capture and recycling, *ChemSusChem*, 2008, **1**, 228–235.

22 D. Román González, A. Moro, F. Burgoa, E. Pérez and M. D. Bermejo Roda, Hydrothermal CO_2 conversion using zinc as reductant: Batch reaction, modeling and parametric analysis of the process, *J. Supercrit. Fluids*, **140**, 320–328.

23 K. Kuroda, Y. Shimada and K. Takahashi, CO2-triggered fine tuning of electrical conductivity via tug-of-war between ions, *New J. Chem.*, 2018, **42**, 15528–15532.

24 S. Ullah, A. Badshah, F. Ahmed, R. Raza, A. Altaf and R. Hussain, Electrodeposited Zinc Electrodes for High Current Zn/AgO Bipolar Batteries, *Int. J. Electrochem. Sci.*, 2011, **6**(9), 3801–3811.

25 S. Alamdari, M. Sasani Ghamsari, C. Lee, W. Han, H.-H. Park, M. J. Tafreshi, H. Afarideh and M. H. M. Ara, Preparation and Characterization of Zinc Oxide Nanoparticles Using Leaf Extract of Sambucus ebulus, *Appl. Sci.*, 2020, **10**, 3620.

26 D. Nguyen, M. Jee, D. H. Won, H. Jung, H.-S. Oh, B. Min and Y. Hwang, Selective CO2 Reduction on Zinc Electrocatalyst: The Effect of Zinc Oxidation State Induced by Pretreatment Environment, *ACS Sustainable Chem. Eng.*, 2017, **5**(12), 11377–11386.

27 R. Kas, K. K. Hummadi, R. Kortlever, P. de Wit, A. Milbrat, M. W. J. Luiten-Olieman, N. E. Benes, M. T. M. Koper and G. Mul, Three-dimensional porous hollow fibre copper electrodes for efficient and high-rate electrochemical carbon dioxide reduction, *Nat. Commun.*, 2016, **7**, 10748.

28 C. Tien-Fu, R. Rajendran, I. E. Kuznetsova and G.-J. Wang, High-power, non-enzymatic glucose biofuel cell based on a nano/micro hybrid-structured Au anode, *J. Power Sources*, 2020, **453**, 227844.

29 Y. Zhao, L. Tian, Y. Fan, M. Zhang and X. Wang, Non-enzymatic glucose biofuel cells based on highly porous PtxNi1-x nanoalloys, *J. Mater. Sci.*, 2021, **56**, 13066–13082.